CHINESE JOURNAL OF MECHANICAL ENGINEERING
Vol. 27, No. 1, 2014

DOI: 10.3901/CJME.2014.01.146, available online at www.springerlink.com; www.cjmenet.com; www.cjmenet.com.cn

Design of Compliant Straight-line Mechanisms Using Flexural Joints

PEI Xu*, YU Jingjun, ZONG Guanghua, and BI Shusheng

School of Mechanical Engineering and Automation, Beihang University, Beijing 100191, China

Received November 21, 2012; revised November 12, 2013; accepted November 13, 2013

Abstract: Straight-line compliant mechanisms are important building blocks to design a linear-motion stage, which is very useful in precision applications. However, only a few configurations of straight-line compliant mechanisms are applicable. To construct more kinds of them, an approach to design large-displacement straight-line flexural mechanisms with rotational flexural joints is proposed, which is based on a viewpoint that the straight-line motion is regarded as a compromise of rigid and compliant parasitic motion of a rotational flexural joint. An analytical design method based on the Taylor series expansion is proposed to quickly obtain an approximate solution. To illustrate and verify the proposed method, two kinds of flexural joints, cross-axis hinge and leaf-type isosceles-trapezoidal flexural(LITF) pivot are used to reconstruct straight-line flexural mechanisms. Their performances are obtained by analytic and FEA method respectively. The comparisons of the results show the accuracy of the approach. Both examples show that the proposed approach can convert a large-deflection flexural joint into approximate straight-line mechanism with a high linearity that is higher than 5 000 within 5 mm displacement. This can lead to a new way to design, analyze or optimize straight-line flexure mechanisms.

Keywords: flexure mechanism; straight-line mechanism; flexural joint; center-shift

1 Introduction

In various fields of application, such as micro-positioning in manufacturing equipment, and accurate measurement in optical systems, there is an urgent need for linear-motion mechanisms[1–3] to perform an ultra-high-precision translational motion. Conventional mechanisms with assembled joints and rigid links cannot meet this demand due to their coarse precision caused by friction, backlash, etc. Generally, the resultant errors are also hardly traded off by controllers and sensors. Compliant mechanisms[4–5] of miniature and monolithic work pieces, instead, could potentially offer an attractive alternative to traditional linear motion mechanisms both in terms of improved functionality and decreased cost.

A flexure mechanism is a kind of precision compliant mechanisms depending on lumped-compliance or distributed-compliance characteristics of flexures among the mechanism. The motion of the flexure mechanisms is achieved via the deflection of these flexures in the mechanism. This kind of mechanism can be designed as a monolithic structure, which makes possible to achieve a high accuracy. Therefore, they have less wear, no backlash and no friction, as well as the potential to realizing large range of motion due to usage of large-deformation flexure elements. Several linear-motion flexure mechanisms, including parallel-guiding flexure mechanisms, have been developed [6–11].

A straight-line mechanism is a mechanism which provides at least a point on its component moving in a straight line[12]. The corresponding rigid straight-line mechanisms include Watt's linkage, Chebyshev linkage, Roberts linkage, and Peaucellier-Lipkin linkage, etc. A linear-motion mechanism, however, provides translational motion of its component, which means there are two or more points on the component. By definition, the linear-motion mechanism is included into straight-line mechanisms. On the other hand, a linear-motion mechanism can be regarded as the combination of two or several straight-line mechanisms as fundamental building blocks. This conclusion is also available for the flexure mechanism family. For example, in a flexural Roberts straight-line mechanism as shown in Fig. 1(a), there is only one point P on the middle link moving in a straight line. Two Roberts mechanisms can compose a linear-motion mechanism as shown in Fig. 1(b). All points on the rigid body P_1P_2 move in a straight line. From this view point, a parallel linear spring stage[13–14] (a linear-motion flexure mechanism) is consisted of two parallel leaf-springs, which can be regarded as combinations of two approximate straight-line mechanisms. As another example, a fully compliant linear-motion mechanism, developed by HUBBARD, et al[15] and termed as "XBob", is made up of eight Roberts mechanisms. In addition, several other kinds of straight-line mechanisms are also involved, such as

* Corresponding author. E-mail: peixu@buaa.edu.cn
This project is supported by National Natural Science Foundation of China (Grant No. 51275552), and Foundation for the Author of National Excellent Doctoral Dissertation of China (Grant No. 201234)

Scott-Russell mechanism[16], which is always used in compliant mechanisms to guide or amplify the output motion.

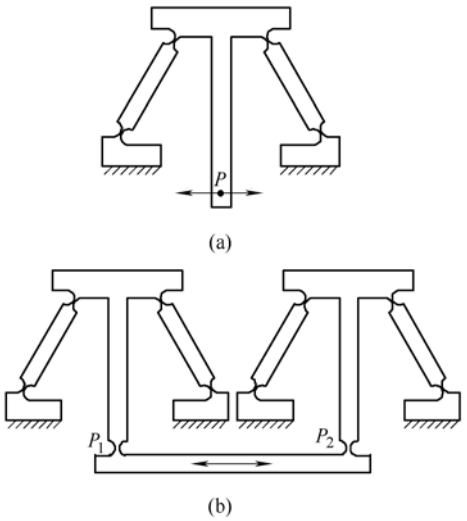

Fig. 1. Flexural straight-line mechanism and linear-motion mechanism

Meanwhile, several systematic approaches to synthesizing straight-line flexure mechanisms were also investigated[17–19]. However, most of them are based on the parallelogram linkage, and ignore the effects of parasitic motion on characteristics of the mechanism. The parasitic motions of a flexure mechanism are trivial enough during a short range of travel to be neglected in the general usages. But some precision applications also requiring a large range of motion, the parasitic motions are always annoying and hard to be eliminated. Traditional elimination solution is usually achieved by parallel connection or symmetric design. The main aim of this approach is trying to restrain the parasitic motion and consequently improve the payload capability and the stiffness characteristic greatly. It also makes the range of motion decreased increasingly. As an alternative of improving this trade-off, one practical way is to meliorate linearity of each straight-line mechanism module. The higher the linearity is, the smaller the disadvantageous effects caused by parallel connection are.

In this paper, we try to design the straight-line mechanisms using the rotational flexural joints. The main idea stems from making full use of the parasitic motion generated by axis-shift (in this paper, it is called compliant parasitic motions) to compensate the trajectory deviation from a straight line (in this paper, it is called rigid parasitic motions) in a simple flexure revolute joint. Although the center-shift of a flexural joint as a disadvantageous factor is diminished in general cases, here we turn to effectively control the magnitude and direction of center-shift to get higher linearity and larger range of motion. It can therefore establish a bridge between flexural joints and compliant straight-line mechanisms. Furthermore, the viewpoint is also helpful to find some new types of straight-line flexure mechanisms and to further provide a convenient way to design and optimize them.

It should be noted that the traditional small-deflection flexural joints, such as notch-type joints are not suitable in this approach, since the center-shift is used to counteract the rigid parasitic motion cannot be too small. Therefore, only large-deflection flexural joints are available. For this purpose, two large-deformation flexural joints, i.e., cross-axis hinge and leaf-type isosceles-trapezoidal flexural (LITF) pivot [20] are investigated as two cases.

2 Counteraction of Rigid and Compliant Parasitic Motion (Design Method)

As well known, for a compliant mechanism with flexures, the rotational flexural joints are the basic elements. Lots of investigations have been involved with the analysis, synthesis and optimization of various flexural joints. If we can start to design a straight-line flexure mechanism from the flexural joints, then the previous works can be used, and new kinds of straight-line flexure mechanisms even may be found by flexural joints.

In order to explain the viewpoint, firstly we classify the parasitic motions of a flexural joint into two categories, i.e. rigid parasitic motion and compliant parasitic motion. The parasitic motion induced by an ideal revolute joint is defined as the rigid parasitic motion here, while the other one only caused by the compliant nature is called the compliant parasitic motion. For example, because of their rotational nature, all the flexural joints can be equivalent to a pin joint as shown in Fig. 2. The corresponding rigid configuration consisted of a pivot and a link. When the rotational angle is small enough, the assembly can be considered as an approximate straight-line mechanism characterizing the straight-line motion near parallel to x-axes at point B of the link. In this case, the motion of point B parallel to y-axe (denoted as d_r) is defined as the rigid parasitic motion. The d_r is given by

$$d_r = H_p(1-\cos\theta)\,, \tag{1}$$

where H_p is the distance between point B and the pivot axes, θ is the rotational angle. d_r can be considered as the error when this mechanism is used to generate a straight line.

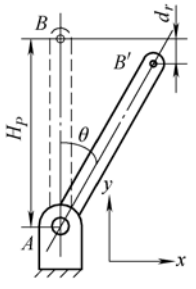

Fig. 2. Rigid parasitic motion of a linkage

By replacing the above rigid pivot with a flexural joint, such as a leaf spring, a corresponding compliant

mechanism is constructed as shown in Fig. 3. The pivot point of the leaf spring is point *O*. For a flexural joint, the center-shift leads to a kind of parasitic motion other than rigid parasitic motion. If the center-shift of the leaf spring is zero (like an ideal joint), point *D* located on the upper rigid part will rotated to the position D_r. However, because of the center-shift *d*, point *D* will move to the position *D*′. The center-shift can be further decomposed into *x*-direction and *y*-direction components. Here the *y*-direction component of the center-shift refers to the compliant parasitic motion, denoted as d_c. The *x*-direction component, d_x, which is along the direction of the line motion (assuming the straight-line motion is parallel to *x*-axes), however, is much smaller than the displacement of point *D*. Hence, we can ignorant the effect of d_x in this case.

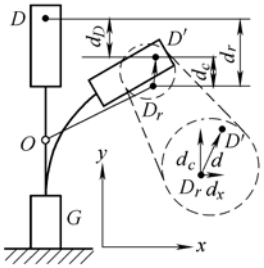

Fig. 3. Compliant parasitic motion of a compliant mechanism

In Fig. 2, the directions of the rigid parasitic motion d_r and compliant parasitic motion d_c are always opposite to each other. Their counteraction just can be used to improve the linearity of the movement of point *D*. If we use this compliant mechanism as a straight-line mechanism, the linearity of the mechanism is largely dependent on the choice of the magnitudes of both d_r and d_c.

In conclusion, to reconstruct a flexural joint to a straight-line mechanism, two conditions should be satisfied.

(1) The directions of the center shift should be opposite against the direction of the rigid parasitic motion.

(2) When the rotational angle θ increase, the magnitude of d_r should be close to d_c. So they can be neutralized.

There are many ways to find answers that can satisfy above two conditions. Here, we give an analytical method to quickly obtain an approximate solution. This method is based on the Taylor series expansion.

Through Taylor series expansion, Eq. (1) can be expressed as

$$d_r = \frac{H_p}{2}\theta^2 - \frac{H_p}{24}\theta^4 + \frac{H_p}{720}\theta^6 - \cdots . \tag{2}$$

It can be written in the form

$$d_r = a_2\theta^2 + a_4\theta^4 + a_6\theta^6 + \cdots . \tag{3}$$

If the center-shift component d_c can also be written in the same form

$$d_c = b_2\theta^2 + b_4\theta^4 + b_6\theta^6 + \cdots . \tag{4}$$

Then we can control the magnitude of a_2 (by adjusting of H_p) and b_2 (by selecting configuration and parameters of flexural joint) to keep

$$a_2 = b_2 , \tag{5}$$

i.e.,

$$H_p = 2b_2 . \tag{6}$$

Therefore, the error of the line motion after the neutralization is

$$\varepsilon = d_c - d_r = (b_4 - a_4)\theta^4 + o(\theta^4) . \tag{7}$$

Because angle θ is very small ($\theta \ll 1$), the terms with higher order in Eq. (7) may be ignored.

3 Design Process

Based on the above viewpoint and method, a systematic process to design a compliant approximate straight-line mechanism can be explicitly described as follows.

Step 1. Select a flexural joint with large-deflection capability.

Step 2. Given a flexural joint, its center-shift should be calculated precisely.

Step 3. If condition (1) can be satisfied and the center-shift can be expanded in the form of Eq. (4), go to the next step. Otherwise, the flexural joint cannot be used to construct a straight-line mechanism.

Step 4. Choose H_p (the corresponding point can be called characteristic point), and adjust the parameters of the flexural joint to ensure the center-shift satisfy Eq. (6).

Step 5. On the rigid bar attached to the mobile part of flexural joint, the characteristic point can move on an approximate straight line when the flexural joint deflects.

Step 6. Based on the results of FEA software or other more precise tools, the position of the characteristic point can be adjusted slightly to further improve the linearity.

The correctness of the result is largely dependent on the accuracy of the center-shift's analysis. The performance of an approximate straight-line mechanism can be evaluate by the linearity λ, which can be defined as

$$\lambda = d_x / d_y , \tag{8}$$

where d_x is the distance that the characteristic point moves along the defined straight line, d_y is the offset perpendicular to d_x. The larger the linearity λ is, the more close to straight-line the trajectory of the characteristic point is.

In the next two sections, two examples are selected to illustrate how the method works. And the results are compared with the FEA method.

4 Case Study I: Cross-axis Hinge

A cross-axis hinge, widely used in applications requiring large deflections[13], consisted of two or more leaf springs each attached to a fixed base at one end and the moving platform at the other, as shown in Fig. 4(a). Although a relatively large center-shift of the flexure is a shortcoming in its application as a rotational joint, it makes the cross-axis hinge available to reconstruct a straight-line mechanism.

Without loss of generality, a cross-axis hinge only consisting of two leaf springs is investigated. The two leaf springs have a uniform-thickness and the same width. The pivot center O is assumed to be on the axis of intersection between the leaf springs (Fig. 4(b)). The distance between O and the moving platform DC is H; the distance between O and the fixed base AB is h_f; the half angle between two leaf springs is φ. The rotational angle of the moving platform DC is θ.

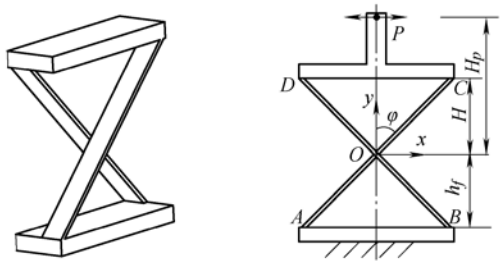

Fig. 4. Cross-axis hinge

According to Ref. [20], the center-shift of a cross-axis hinge outline in Fig. 4b is given by

$$\delta_x = -B_1 \bullet H \sin\theta , \tag{9}$$

$$\delta_y = B_1 \bullet \left(\cos\theta - 1 + \frac{\gamma}{n}\right) H , \tag{10}$$

where γ is the characteristic radius factor, and

$$B_1 = \tan\varphi \sqrt{\frac{B_3}{B_2} - 1} - 1 , \tag{11}$$

$$B_2 = \gamma^2 - 2(\gamma - n) n (1 - \cos\theta) , \tag{12}$$

$$B_3 = \gamma^2 / \sin^2\varphi , \tag{13}$$

$$n = \frac{H}{H + h_f} , \tag{14}$$

$$\gamma = \frac{15n^2}{2 - 3n + 18n^2} . \tag{15}$$

Substitute Eqs. (11)–(15) into Eq. (10), and solve the equation

$$\delta_y > 0 , \tag{16}$$

i.e.,

$$h_f > (7 - 3\sqrt{5}) H / 2 = 0.145\,9H . \tag{17}$$

Generally, h_f satisfies Eq. (2). So the cross axis hinge can satisfy condition (1).

The Taylor series expansion of Eq. (10) yields

$$\delta_y = \frac{H(\gamma - n)}{2\gamma \cos^2\varphi}\theta^2 - \frac{H(\gamma - n)\left[3\gamma n - 3n^2 + \left(\gamma^2 - 6\gamma n + 12n^2\right)\cos^2\varphi\right]}{24\gamma^3 \cos^4\varphi}\theta^4 + \cdots , \tag{18}$$

thus the cross axis hinge satisfies condition (2).

Eq. (6) is written as

$$H_p = \frac{\gamma - n}{\gamma \cos^2\varphi} H . \tag{19}$$

If the characteristic point P locates on the moving platform or outside of the hinge, then H_p should be larger H, i.e.,

$$\frac{\gamma - n}{\gamma \cos^2\varphi} \geqslant 1 . \tag{20}$$

The error of the line motion defined by Eq. (7) yields

$$\varepsilon = \frac{n(\gamma - n)\left[n - \gamma + 2(\gamma - 2n)\cos^2\varphi\right]}{8\gamma^3 \cos^4\varphi} H\theta^4 . \tag{21}$$

The displacement of the line motion is given by

$$d_x = H_p \sin\theta + \delta_x \approx H_p \theta . \tag{22}$$

The linearity defined by Eq. (8) yields

$$\lambda = \frac{d_x}{\varepsilon} = \frac{8\gamma^2 \cos^2\varphi}{n\left[\gamma - n - 2(\gamma - 2n)\cos^2\varphi\right]\theta^3} . \tag{23}$$

The maximum deflection of the cross-axis hinge is given by

$$\theta_{\max} = \frac{H}{Et(3n - 1)n\cos\varphi} d_c , \tag{24}$$

where t is the thickness of the leaf-type segments, E is the Young's modulus. Thus the maximum range of motion of the straight-line mechanism is

$$d_{\max} = H_p \sin\theta_{\max} . \tag{25}$$

In most occasions, the symmetric shape is preferred, then we can select $H=h_f$,

$$n = 1/2 , \tag{26}$$

$$\gamma = 3/4 . \tag{27}$$

Hence, Eq. (20) reduces to

$$\frac{1}{3\cos^2\varphi} \geqslant 1 , \tag{28}$$

when $\varphi > \arccos\sqrt{3}/3 = 54.735\,6°$, the inequality in Eq. (28) is tenable.

Also, Eqs. (19), (21), (23) and (24) reduce to

$$H_p = \frac{1}{3\cos^2\varphi} H , \tag{29}$$

$$\varepsilon = \frac{2\cos^2\varphi + 1}{108\cos^4\varphi} H\theta^4 , \tag{30}$$

$$\lambda = \frac{36}{\left(2 + \dfrac{1}{\cos^2\varphi}\right)\theta^3} , \tag{31}$$

$$\theta_{\max} = \frac{4H}{Et\cos\varphi} d_c . \tag{32}$$

Then we can select proper parameters to obtain a large stroke ($d_{\max}$) and a high linearity (λ).

The following concrete example uses FEA to validate the approach. Selecting φ=60°, H=30 mm, h_f=H, t=0.5 mm, b=5 mm (b is the thickness of the pivot) then

$$H_p = 40 \text{ mm} , \tag{33}$$

$$\varepsilon = \frac{2}{9} H\theta^4 , \tag{34}$$

$$\lambda = \frac{6}{\theta^3} . \tag{35}$$

The numerical simulation is made with a commercial FEA program ANSYS capable of nonlinear analysis. The Beam elements were used with the large displacement option turned on. The material assumed in these cases is Aluminum alloy. The Young's modulus, E, is chosen 71 GPa and the Poisson's ratio is 0.33.

The cross-axis hinge is fixed as shown in Fig. 4(b), and a moment is applied on the middle of movable segment. The movement trace of the characteristic point P is recorded. Fig. 5 shows the displacement of point P in y-direction error motion, ε, vs. the displacement in x-direction, d_x. The analytic results are illustrated in the figures. The curves show that the analytical method predicts the movement of the characteristic point pretty well. When the displacement of x-direction is less than 5 mm, the error of line motion is less than 0.001 mm, therefore, the linearity is higher than 5 000. When the displacement of x-direction increases, the linearity drops quickly.

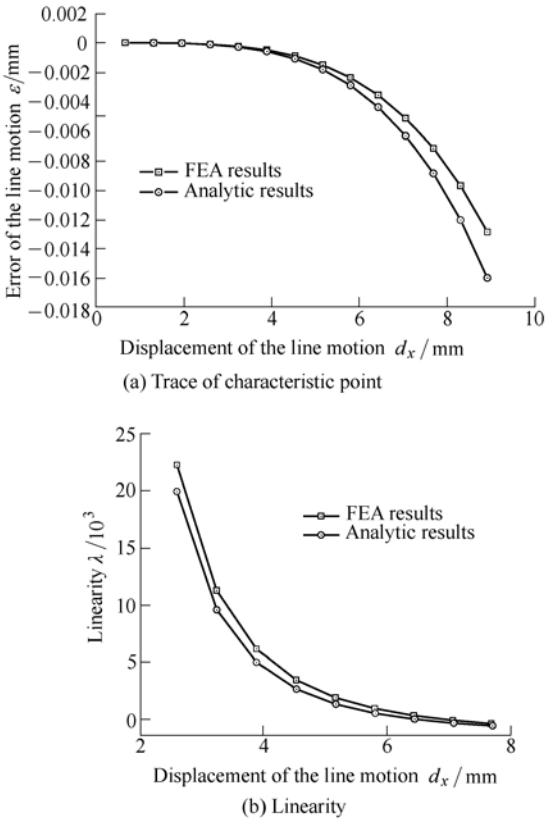

Fig. 5. Displacement of point P in a cross-axis hinge

In order to illustrate the efficiency of the method, the parallel linear spring stage is introduced to compare with the approximate straight-line mechanism derived from the cross-axis hinge, as shown in Fig. 6. The parameters of the parallel linear spring stage are: l=60 mm, t=0.5 mm, b=5 mm. In the figures, it can be seen that the movement of the characteristic point of the cross-axis hinge is much close to a straight-line than the parallel linear spring stage. When the displacement of x-direction is 5 mm, the linearity of the cross-axis hinge is 5 000, while the linearity of the parallel linear spring stage is only 20.

The accuracy of result obtained by the method is relied on the accuracy of the calculation of center-shift. The finite element model can be used to optimize the line motion further to make the linearity higher.

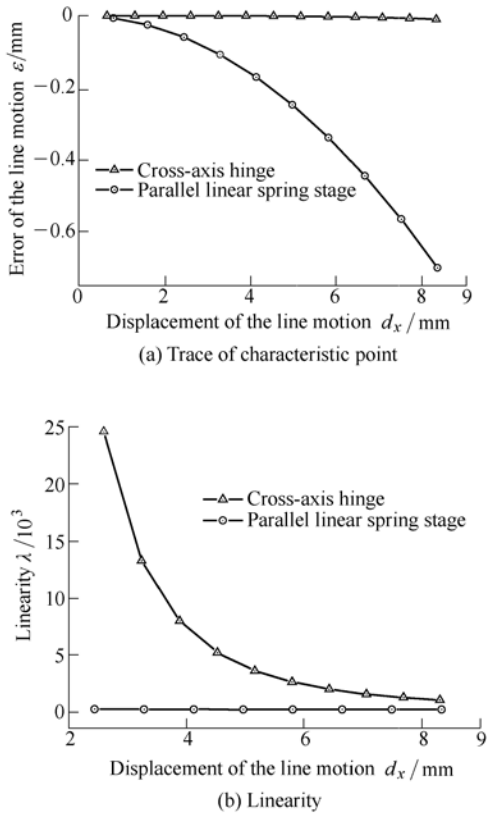

Fig. 6. Comparisons between the cross-axis hinge and parallel linear spring stage

5 Case Study II: LITF Pivot

A LITF pivot is a type of large-deflection flexural joint, which always can be used as a building block to construct new large-deflection high-precision flexural joints, such as Cartwheel hinge and butterfly flexural joint. Also, the center-shift of a single LITF pivot is relatively large; it therefore can be used to reconstruct an approximate straight-line mechanism, i.e., roberts mechanism.

The LITF pivot consists of two leaf-type segments and two rigid segments (Fig. 6). The lengths of two leaf-type segments are identical. In the initial unloaded configuration, the two rigid segments are parallel to each other. Thus the configuration of a LITF pivot can be completely determined by three parameters: (1) h_f denotes the distance between the bottom AB and the virtual pivot point O; (2) H denotes the distance between bottom DC and point O; (3) φ denotes half of the angle between two sides.

The analysis of the LITF pivot by the PRB model is proposed in literatures[19–20]. If the long base of a LITF pivot (DC in Fig. 7) is fixed, then the short one (AB) can move around point O. Its y-direction component of the center-shift can be given by

$$\delta_y = \left[1-\left(1-\frac{\gamma}{n}\right)\cos\theta\right]B_1 H\,, \tag{36}$$

where B_1 is obtained by Eq. (11), the characteristic radius factor γ can be computed by Eq. (15). Because the direction of h_f is opposite to one of the cross-axis hinge, the value of n in Eq. (14) becomes

$$n = \frac{H}{H-h_f}\,. \tag{37}$$

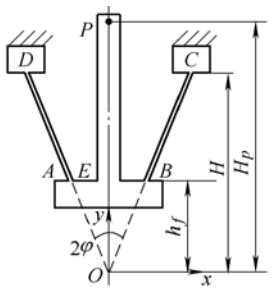

Fig. 7. LITF pivot to generate a straight-line motion at point P (Roberts mechanism)

Eq. (37) indicates $n \geqslant 1$. Since γ, n and $\cos\theta$ are larger than zero respectively, then $\delta_y > 0$, i.e., the LITF pivot can satisfy condition (1).

The Taylor series expansion of Eq. (36) is

$$\delta_y = \frac{H(n-\gamma)}{2\gamma\cos^2\varphi}\theta^2 - \frac{H(\gamma-n)\left[3\gamma n-3n^2+(7\gamma^2-18\gamma n+12n^2)\cos^2\varphi\right]}{24\gamma^3\cos^4\varphi}\theta^4+\cdots. \tag{38}$$

Thus the cross axis hinge satisfies condition (2).

Attaching a rigid segment on the movable segment DC, such as bar EP in Fig. 7, the characteristic point P is located on the y-axis in the initial position. The distance between point P and center O, H_p, can be calculated by solving Eq. (6)

$$H_p = \frac{n-\gamma}{\gamma\cos^2\varphi}H\,. \tag{39}$$

If the characteristic point P should locate on the moving platform or outside of the hinge, then H_p should be larger H, i.e.,

$$\frac{n-\gamma}{\gamma\cos^2\varphi} \geqslant 1\,, \tag{40}$$

i.e.,

$$\frac{2(9n^2-9n+1)}{15n\cos^2\varphi} \geqslant 1\,. \tag{41}$$

The results will be

$$n \geqslant \frac{1}{12}\left[6+5\cos^2\varphi+\sqrt{5(5\cos^4\varphi+12\cos^2\varphi+4)}\right]. \tag{42}$$

Therefore, condition (3) can be satisfied.

The error of the line motion defined by Eq. (7) yields

$$\varepsilon = \frac{(\gamma - n)^2 \left[3n - 2\gamma + 2(\gamma - 2n)\cos^2\varphi\right]}{8\gamma^3 \cos^4\varphi} H\theta^4 . \quad (43)$$

The linearity defined by Eq. (8) yields

$$\lambda = \frac{8\gamma^2}{(\gamma - n)(2\gamma - 4n + n/\cos^2\varphi)\theta^3} . \quad (44)$$

The maximum range of motion of the constructed straight-line mechanism is also given by Eqs. (24) and (25).

In the next, a concrete example is designed to validate the equations. Selecting h_f=8.75 mm, H=20 mm, φ=30°, t=0.5 mm, b=5 mm. According to Eq. (10), H_p=26.89 mm. The parameters setting in ANSYS is the same as those of section 4. The LITF pivot is placed as shown in Fig. 7, and a lateral force is loaded on the characteristic point P. The displacements of point P are recorded as shown in Fig. 8a. The analytic results computed by Eq. (43) are also illustrated in the Figure. The two curves are close to each other, which prove the correctness of the approach. The linearity of point P is shown in Fig. 8(b). When d_x is lesser than about 3.5 mm, the linearity is larger than 1 000, which means that the LITF pivot can be used as an approximate straight-line mechanism with a high linearity within a relatively large stroke.

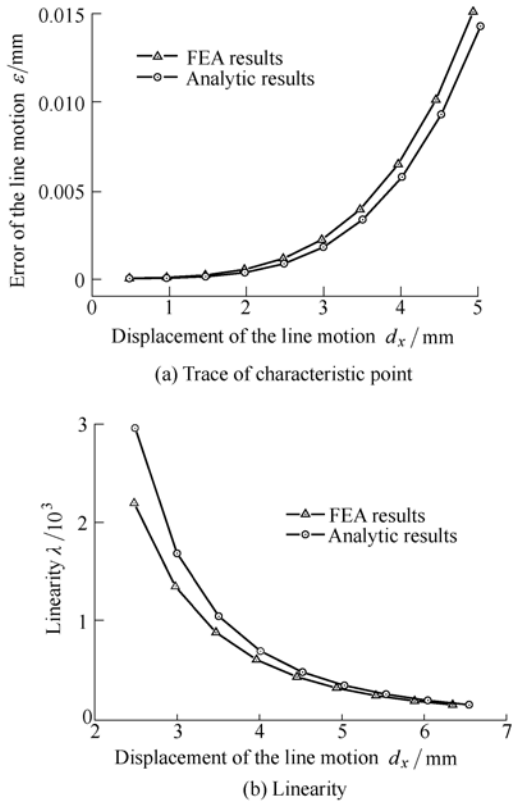

Fig. 8. Displacement of point P on the LITF pivot

6 Conclusions

(1) A new viewpoint is proposed to convert rotational flexural joints into straight-line flexural mechanisms in the view of exploiting the parasitic motions. After taking advantage of the previous investigations on rotational flexural joints, a new type of straight-line mechanisms can be obtained by counteracting both the rigid and compliant parasitic motion. Such a viewpoint establishes a bridge between rotational flexural joints and straight-line mechanisms, and lead to a new way to design, analyze or optimize straight-line flexure mechanisms.

(2) An analytical design method based on the Taylor series expansion is deduced to quickly obtain an approximate solution. To illustrate and verify the proposed method, two kinds of flexural joints, cross-axis hinge and LITF pivot are used to reconstruct straight-line flexural mechanisms. The results verified by FEA method shows the calculated model is accurate. Both examples show that the proposed method can derive a large-deflection flexural joint into approximate straight-line mechanism with a high linearity (higher than 5 000 within 5 mm displacement).

It should be noted that the accuracy of the result is largely relied on the accuracy of the calculation of center-shift when using the method. Thus the finite element model can be used to further optimize the straight-line mechanism.

References

[1] SLOCUM A H. Precision machine design[M]. *Society of Manufacturing Engineers*, Dearborn, MI, 1992.

[2] PARISE J J, HOWELL L L, MAGLEBY S P. Ortho-planar linear-motion springs[J]. *Mechanism and Machine Theory*, 2001, 36(11): 1 281–1 299.

[3] ZHAO S, AYE Y N, SHEE C Y, et al. A compact 3-DOF compliant serial mechanism for trajectory tracking with flexures made by rapid prototyping[C]//*2012 IEEE International Conference on Robotics and Automation*, Minnesota, USA, May 14–18, 2012.

[4] HOWELL L L. Compliant mechanisms[M]. *Wiley-interscience Publication*, 2001.

[5] CANFIELD S L, BEARD J. Development of a spatial compliant manipulator[J]. *International Journal of Robotics and Automation*, 2002, 17(1): 63–71.

[6] AWTAR S, SLOCUM A H. Characteristics of beam-based flexure modules[J]. *ASME Journal of Mechanical Design*, 2007, 129: 625–638.

[7] CHOI K B, KIM D H. Monolithic parallel linear compliant mechanism for two axes ultraprecision linear motion[J]. *Review of Scientific Instruments*, 2006, 77: 065106.

[8] YU Jingjun, HU Yida, BI Shusheng, et al. Kinematics feature analysis of a 3 DOF in-parallel compliant mechanism for micro manipulation[J]. *Chinese Journal of Mechanical Engineering*, 2004, 17(1): 127–131.

[9] TANG X, CHEN I M, LI Q. Design and Nonlinear Modeling of a Large-Displacement XYZ Flexure Parallel Mechanism with Decoupled Kinematic Structure[J]. *Review of Scientific Instruments*, 2006, 77: 115101.

[10] GAROI F, WINTERFLOOD J, JU L, et al. Passive vibration isolation using a roberts linkage[J]. *Review of Scientific Instruments*,

2003, 74(7): 3 487.

[11] ROMAN G A, WIENS G J. MEMS optical force sensor enhancement via compliant mechanism[C]//*ASME IDETC/ CIE2007*, Las Vegas, Nevada, USA, 2007.

[12] KEMPE A B. *How to draw a straight line: a lecture on linkages*[M]. Macmillan and Co, 1877.

[13] SMITH S T. *Flexures: elements of elastic mechanisms*[M]. New York: Gordon and Breach Science, Amsterdam, The Netherlands, 2000.

[14] HOPKINS J B, CULPEPPER M L. Synthesis of multi-degree of freedom, parallel flexure system concepts via freedom and constraint topology (FACT). Part II: Practice[J]. *Precision Engineering*, 2010, 34(2): 271–278.

[15] HUBBARD N B, WITTWER J W, KENNEDY J A. A novel fully compliant planar linear-motion mechanism[C]//*Proc. ASME DETC'04*, Utah, USA. 2004.

[16] CHANG S, DU B. A precision piezodriven micropositioner mechanism with large travel range[J]. *Review of Scientific Instruments*, 1998, 69(4): 1 785.

[17] LIN Y T, LEE J J. Structural synthesis of compliant translational mechanisms[C]//*12th IFToMM World Congress*, Besançon, France. 2007.

[18] TREASE B P, MOON Y M, KOTA S. Design of large-displacement compliant joints[J]. *Journal of Mechanical Design*, 2005, 127: 788.

[19] PEI X, YU J J, ZONG G H, et al. Analysis of rotational precision for an isosceles-trapezoidal flexural pivot[J]. *Journal of Mechanical Design*, 2008, 130(5): 052302.

[20] PEI X, YU J J, ZONG G H, et al. A novel family of leaf-type compliant joints: combination of two isosceles-trapezoidal flexural pivots[J]. *Journal of Mechanisms and Robotics*, 2009, 1(2): 021005.

Biographical notes

PEI Xu, born in 1979, is currently a lecturer at *School of Mechanical Engineering and Automation, Beihang University, China*. He received his PhD degree from *Beihang Universtiy, China*, in 2009. His main research interests include Parallel mechanisms, compliant mechanisms, and robotics.
Tel: +86-10-82317745; E-mail: peixu@buaa.edu.cn

YU Jingjun, born in 1974, is currently an associate professor at *Robotics Institute, Beihang University, China*. He received his PhD degree from *Beihang Universtiy, China*, in 2002. His main research interests include Parallel mechanisms, compliant mechanisms, robotics and screw theory.
Tel: +86-10-82338019; E-mail: jjyu@buaa.edu.cn

ZONG Guanghua, born in 1943, is currently a professor at *Robotics Institute, Beihang University, China*. His research interests include compliant mechanisms, mobile robots, etc.
Tel: +86-10-82338916; E-mail: ghzong@buaa.edu.cn

BI Shusheng, born in 1966, is currently a professor at *Robotics Institute, Beihang University, China*. He received his PhD degree from *Beihang University, China*, in 2002. His research interests include bionic under water robots, bird-like robots, and flexible micro-structure design.
Tel: +86-10-82338926; E-mail: biss_buaa@163.com